

# NUMERICAL MODELLING OF WIND LOADS. VERIFICATION AND VALIDATION FOR THE KEMEROVO MUSEUM, THEATRE AND EDUCATION COMPLEX

*Alexander M. Belostotsky, Oleg S. Goryachevsky, Sergey G. Saiyan,  
Alexandra M. Efimova*

National Research Moscow State University of Civil Engineering, Moscow, RUSSIA

**Abstract:** This paper presents the results of numerical modelling of mean and peak pressure coefficients for a unique facility, conducted within the verification procedure of Ansys Fluent in the RAASN system. The applicability of the steady-state (RANS) simulations and three turbulence models (SST  $k-\omega$ , EARSM, GEKO  $k-\omega$ ) is verified for the wind loads determination. The results are compared against experimental data obtained in the MSUCE wind tunnel. The weak applicability of often recommended methods of grid extrapolation (Richardson extrapolation and approximate error spline) is revealed. It is shown that the GEKO  $k-\omega$  turbulence model with the separation parameter  $C_{SEP} = 1.25$  provides a better fit to the wind tunnel data than SST  $k-\omega$  and EARSM.

**Keywords:** computational fluid dynamics (CFD), wind loads, verification, validation, Richardson extrapolation, Approximate Error Spline

## ВЕРИФИКАЦИЯ И ВАЛИДАЦИЯ ЧИСЛЕННОГО МОДЕЛИРОВАНИЯ ВЕТРОВЫХ НАГРУЗОК НА ПРИМЕРЕ МУЗЕЙНОГО И ТЕАТРАЛЬНО-ОБРАЗОВАТЕЛЬНОГО КОМПЛЕКСА В Г. КЕМЕРОВО

*А.М. Белостоцкий, О.С. Горячевский, С.Г. Саиян, А.М. Ефимова*

Национальный исследовательский Московский государственный строительный университет, г. Москва, РОССИЯ

**Аннотация:** Для уникального здания представлены результаты численного моделирования аэродинамических коэффициентов средних и пиковых давлений, полученные в рамках процедуры верификации в системе RAACH программного комплекса ANSYS Fluent. Проверяется применимость для определения ветровых нагрузок стационарной постановки (RANS) и трёх моделей турбулентности: SST  $k-\omega$ , EARSM, GEKO  $k-\omega$ . Результаты сопоставляются с экспериментальными данными, полученными в аэродинамической трубе НИУ МГСУ. Выявлена слабая применимость часто рекомендуемых методов сеточной экстраполяции: метода Ричардсона и аппроксимации ошибки сплайном. Выявлено, что модель турбулентности GEKO  $k-\omega$  с параметром  $C_{SEP} = 1.25$  позволяет получить лучшее соответствие данным из аэродинамической трубы, чем SST  $k-\omega$  и EARSM.

**Ключевые слова:** вычислительная аэродинамика, ветровая нагрузка, верификация, валидация, экстраполяция Ричардсона, аппроксимация ошибки сплайном

### 1. INTRODUCTION

Reliable and efficient methods of wind loads determination for buildings and structures is still an urgent task. Mass construction of unique and architecturally outstanding facilities in dense urban

areas stimulates the search for new approaches to solving this problem.

Currently, the following methods are used to determine wind loads:

1. Engineering normative and analytical methods (do not meet the needs of modern construction);

2. Physical modelling in wind tunnels (WTs) [1,2];
3. Numerical modelling [3-11];
4. Monitoring and in-situ measurements [12] (suitable for academic research only);
5. Machine learning and neural networks [13] (under study and yet unapplicable to design).

Physical (experimental) modelling in WT's is currently the most used method to determine wind loads. In the middle of the XX century, an appropriate methodology was developed and validated with in-situ measurements that provides a sufficient level of plausibility under a number of limitations. Still, the high costs of construction and maintenance of WT's, poor scalability, significant experimentation time, low information content and other limitations gradually reduce the role of physical modelling in practice.

Numerical modelling (using CFD), on the other hand, appears to be a more prospective direction: it is devoid of the WT limitations and promises potentially faster research. Therefore, it has already been limitedly legitimised in the regulations of technologically advanced countries [14], STO [15], ASCE 7-22.

For the time of transition from physical to numerical modelling, the most reliable approach is a hybrid one, which means a synthesis of numerical and physical modelling [15].

Currently, the best fit to experimental data is shown by utilising the LES turbulence model. However, its high computational costs hamper its application outside of specialised computational clusters.

Therefore, steady-state (RANS-based) approaches [16] remain the most used ones for fast wind loads determination.

In any case, verification and validation (V&V) procedures are required to confirm the reliability of numerical modelling results. The most general definitions of V&V are given in GOST [17] and ASME [18], but they do not regulate specific procedures and features of individual applications, such as structural aerodynamics.

Due to the lack of exact solutions of mathematical models, *verification* in applications to structural aerodynamics is reduced to evaluating the errors of the numerical model (iteration, time, grid, etc.) [19-21,15].

To assess the grid convergence, a number of sources [19,22-27] recommend the use of such methods, as Richardson extrapolation and approximate error spline. In the present paper, it is shown that these methods do not provide any advantages to the wind loads determination problem.

The *validation* procedure in structural aerodynamics is more straightforward and complies with [17, 18], but it has one peculiarity: in the vast majority of cases, the results of numerical modelling can only be compared with experimental data from WT's.

In the present paper the V&V procedure of the numerical modelling was carried out for a unique facility, the Museum, Theatre and Education Complex (MTEC) in Kemerovo. Three turbulence models were used: SST  $k-\omega$ , EARSM, GEKO  $k-\omega$  (with the separation parameter  $C_{SEP} = 1.25, 1.75, 2.25$ ). Iteration convergence and three mesh variants were investigated.

The results of numerical modelling are compared against experimental data obtained in the MSUCE WT.

The work was carried out within the verification procedure of Ansys Fluent for the problems of "determination of wind and snow actions on buildings and structures on the basis of numerical solutions of the equations of aero-hydrodynamics" in the system of the Russian Academy of Architecture and Construction Sciences (RAASN) [28].

## 2. OBJECT AND METHODOLOGY

### 2.1 Object and task description

In the present paper, a unique facility of the Museum, Theatre and Education Complex (MTEC) in Kemerovo (Fig. 1) was investigated.



*Figure 1. Renders of the MTEC in Kemerovo*

MTEC has a complex deconstructivist shape. Façades combine glass and metal elements. The building has 10 floors with a total area of ~81100 m<sup>2</sup> and an underground car park. The MTEC is planned to house branches of the Mariinsky Theatre and the State Russian Museum, as well as the Kuzbass Arts Centre. The ensemble of the facility is conceived of four parts: a “floating” theatre “cloud”, two “crystals” (a museum and an art centre with workshops), and a public foyer.

The paper investigates the mean ( $c_e$ ) and peak ( $c_{e,+}$ ,  $c_{e,-}$ ) pressure coefficients at control points on the façade and roof of the facility (Fig. 3):

$$c_e = \frac{\Delta\bar{p}}{Q_{ref}}; c_{e,+} = \frac{\Delta\bar{p} + \theta_+ \sigma_p}{Q_{ref}}; c_{e,-} = \frac{\Delta\bar{p} - \theta_- \sigma_p}{Q_{ref}} \quad (1)$$

where  $\Delta\bar{p} = \bar{p} - p_{ref}$  is the pressure drop;  $Q_{ref}$  is the reference wind pressure;  $\sigma_p$  is the standard deviation of pressure;  $\theta_{+(-)}$  are the reliability coefficients.

In the experiment,  $\theta_{+(-)} = 3$ , and  $\sigma_p$  is calculated using a known formula from statistics. In the numerical simulations, these parameters are determined using the methodology for steady-state modelling outlined in [8,16].

The simulations were carried out for the two most typical wind directions (15°, from the surrounding buildings, and 180°, from the unobstructed side, Fig. 2).

Experimental values of pressure coefficients were obtained in the MSUCE WT through physical modelling at a 1:200 scale (Fig. 3).

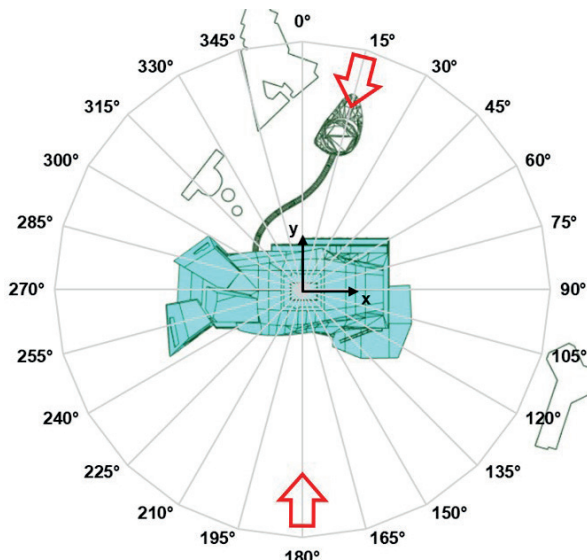


Figure 2. Investigated wind directions



Figure 3. MTEC model in the MSUCE WT (control points are coloured white)

## 2.2 Mathematical models

In the present paper, the calculation of wind flow and wind actions is reduced to the numerical solution of time-averaged (RANS) three-dimensional nonlinear Navier-Stokes equations. For the determination of wind loads and actions on buildings and structures with practically justified simplification the wind flow is assumed to be incompressible and isothermal, and external mass forces are omitted [10]:

$$\frac{\partial \bar{u}_i \bar{u}_j}{\partial x_j} = -\frac{1}{\rho} \frac{\partial}{\partial x_i} \left( \bar{p} + \frac{2}{3} \rho k \right) + \frac{\partial}{\partial x_j} \left( (v + \nu_t) \left( \frac{\partial \bar{u}_i}{\partial x_j} + \frac{\partial \bar{u}_j}{\partial x_i} \right) \right), \quad (2)$$

where  $\bar{u}_i$  are the components of the averaged flow velocity, [m/s];  $t$  is the time, [s];  $\bar{p}$  is the averaged pressure, [Pa];  $\rho = 1.225 \text{ kg/m}^3$  is the air density;  $\nu = 1.46 \cdot 10^{-5} \text{ m}^2/\text{s}$  is the kinematic viscosity of air;  $\nu_t$  is the turbulent viscosity. The continuity equation is given as:

$$\frac{\partial \bar{u}_j}{\partial x_j} = 0 \quad (3)$$

The following turbulence models are considered:

- Shear-Stress Transport (SST)  $k-\omega$  is a widely used two-parameter model that combines the advantages of  $k-\omega$  and  $k-\epsilon$  models for more accurate prediction of turbulent flows. A mixing function [29] is used to transition from the  $k-\omega$  formulation near the boundaries to the  $k-\epsilon$  formulation in the free flow;
- GEKO  $k-\omega$  (Generalised  $k-\omega$ ) is a two-parameter turbulence model developed by Ansys. It is based on the classic Wilcox  $k-\omega$  formulation, but rewritten in a “generalised” form: all dimensional and dimensionless constants are replaced by special functions that are controlled through the model parameters to adjust for different types of flow. In this paper, the parameter  $C_{SEP}$  (equal to 1.25, 1.75 or 2.25), which governs the

adverse pressure gradients and flow separation [29], is varied.

– Explicit Algebraic Reynolds Stress Model (EARSM) is an extension of the standard two-parameter model derived from the Reynolds stress transport equations to account for the non-linear relationship between the Reynolds stresses, the mean strain rate tensor and the vorticity tensor. WJ-BSL-EARSM extends the BSL model to account for the following effects [29]:

- Anisotropy of Reynolds stresses;
- Secondary flows.

### 2.3 CFD models

In order to correctly compare the results of numerical and physical modelling, the CFD model reproduces the main parameters of the experiment: the scale, the dimensions of the WT's working area section, and the boundary conditions.

The numerical geometry of the MTEC with the surrounding buildings totally corresponds to the experimental one (Fig.4).

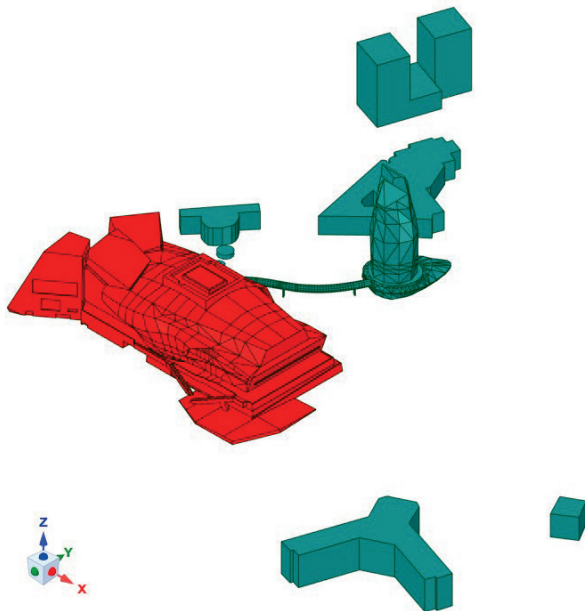


*Figure 4. Geometric model of the facility with the surrounding building in Ansys SpaceClaim*

Finite-volume meshes were created in Ansys Fluent Meshing using polyhexcore method and

combine polygonal, prismatic and cubic finite volumes. Three meshes were developed to analyse the mesh independence of the solution and verify the CFD model: a coarse one (3.1 million cells), a basic one (5.6 million cells, Fig. 6), and a fine one (12.8 million cells). All meshes are similar to each other and differ only in the size of the cells by a factor of 1.5. The number of prismatic layers in the boundary layer is 5 for the coarse mesh, 7 for the basic mesh and 10 for the fine mesh.

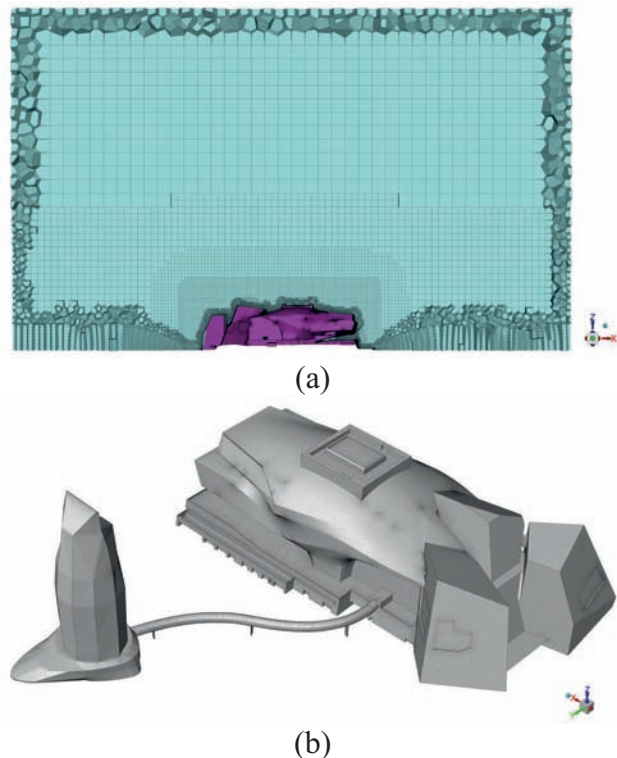


*Figure 5. Finite-volume mesh: a – in the cross-section of the domain; b – on the surface of MTEC and hotel with an elevated bridge*

The boundary conditions are shown in Fig. 6:

- at the inlet, a flow velocity profile and turbulent characteristics are set according to the experimental data from the WT (Fig. 7);
- a free outlet with zero additional pressure;
- at the upper, lower, lateral boundaries and surfaces of the facility and surrounding buildings, a no-slip wall condition is set.

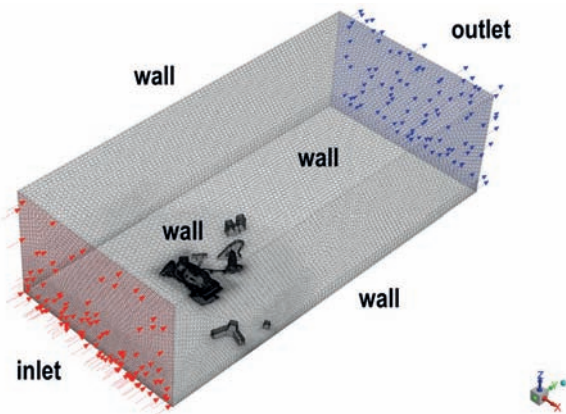


Figure 6. Boundary conditions

A total of 30 3D steady-state simulations (2 angles of attack  $\times$  3 finite-volume meshes  $\times$  5 turbulence models) were performed using Ansys Fluent (see Section 2.2).

The coupled velocity-pressure scheme and 2<sup>nd</sup> order schemes were used for the momentum, turbulent transport and pressure equations. The total number of iterations was set to 700, of which the first 200 were calculated with the time scale factor equal to 1.0, while the next 500 were calculated with the said factor reduced to 0.25.

Data sampling for the iteration convergence analysis was performed on the last 100 iterations.

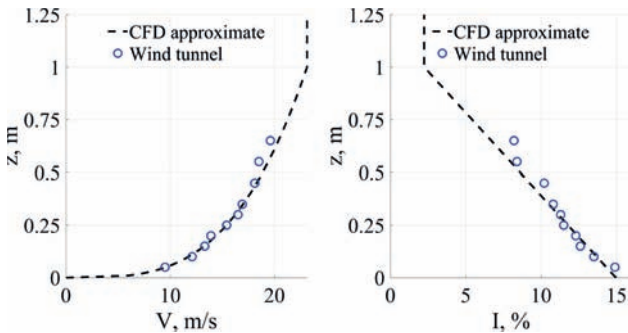


Figure 7. Velocity [m/s] and turbulence intensity [%] profile from WT measurements and CFD approximations

## 2.4 Verification methods

A combined approach, based on two methods outlined in [21-27], was used to estimate the spatial discretisation error: Richardson Extrapolation (RE) and Approximate Error Spline (AES).

The *Richardson extrapolation* suggests extrapolating the investigated parameter to an infinitesimal grid ( $h \rightarrow 0$ ) using the values obtained on a number of finite grids ( $h_1 = h$ ,  $h_2 = \alpha_1 h$ ,  $h_3 = \alpha_2 h$ ). When the coefficient  $\alpha$  is equal to both  $\alpha_1$  and  $\alpha_2$  (in this paper, to 1.5), we get:

$$\varepsilon_1 = \phi_{\alpha h} - \phi_h, \quad \varepsilon_2 = \phi_{\alpha^2 h} - \phi_{\alpha h}, \quad (4)$$

$$p = \frac{\ln|\varepsilon_2/\varepsilon_1|}{\ln(\alpha)} \in [1; 2], \quad (5)$$

$$\phi_{ext} = \frac{\alpha^p \phi_h - \phi_{\alpha h}}{\alpha^p - 1} \quad (6)$$

where  $\phi_h$ ,  $\phi_{\alpha h}$ ,  $\phi_{\alpha^2 h}$  are the values of the sought parameters on the fine, basic and coarse finite-volume grid, respectively;  $p$  is the order of the generalised numerical scheme used for extrapolation;  $\phi_{ext}$  is the extrapolated value ( $h \rightarrow 0$ ).

Application of this method showed that the parameter  $p$  often reaches unrealistic values, resulting in inadequate values of  $\phi_{ext}$ . Therefore, as recommended by the authors, the values of  $p$  were restricted in the range of 1.0 to 2.0.

To estimate the range of grid error, Roache [26-27] proposed the Grid Convergence Index (GCI) (formula 7), which characterises the measure of discrepancy between the numerical result on the fine mesh and the asymptotic value, as well as indicates the behaviour of the numerical solution during further refinement of the finite-volume mesh. When the GCI value is small, the solution is within the asymptotic range:

$$GCI = 1.25 \frac{e_A}{\alpha^p - 1}, \quad (7)$$

where  $e_A = \left| \frac{\phi_h - \phi_{\alpha h}}{\phi_h} \right|$  is the relative approximation error.

*Approximate Error Spline* method [25] assumes the proportionality between the error from the solution  $E_T$  and the error between the numerical solutions  $E_A$ :

$$E_T = \phi - \phi_h, \quad E_A = \phi_h - \phi_{\alpha h}, \quad (8)$$

$$E_T = \beta E_A \quad (9)$$

where  $\phi$  is the unknown exact solution. According to [25], for  $\phi = \phi_{ext}$ :

$$\phi_{ext} = \phi_{\alpha^2 h} + \beta(\phi_{\alpha^2 h} - \phi_{\alpha h}) \quad (10)$$

$$\beta = \frac{1}{2} \frac{\phi_{\alpha^2 h} - \phi_h}{\phi_{\alpha^2 h} - 2\phi_{\alpha h} + \phi_h}. \quad (11)$$

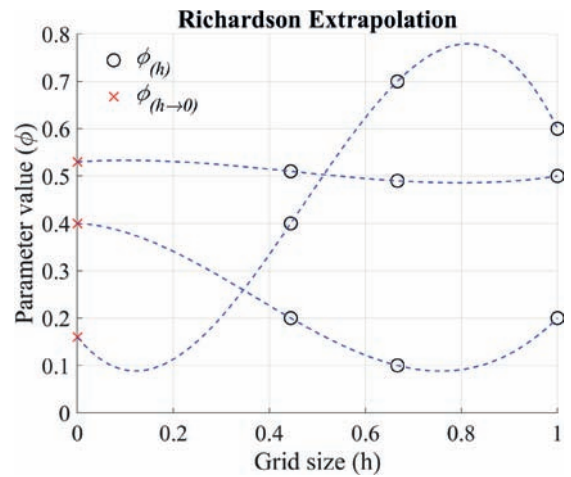
The developers of AES [24] do not provide any methods to estimate the error of the obtained extrapolation. Since in the present work the AES method is used only for oscillatory convergence (see below), we propose to use the  $3\sigma$  rule on the values obtained on three grids:

$$\sigma_\phi = \sqrt{\frac{1}{2} \sum_{i=0}^2 (\phi_{\alpha^i h} - \bar{\phi})^2}, \quad (12)$$

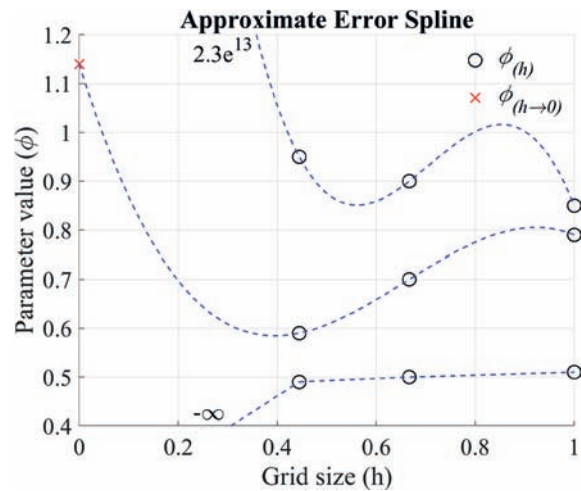
where  $\bar{\phi} = \frac{1}{3} \sum_{i=0}^2 \phi_{\alpha^i h}$  is the average value on the three grids.

Fig. 8 demonstrates the behaviour of the RE and AES methods for typical possible situations. As can be seen from the results, the AES method gives incorrect predictions for monotone convergence and tends to infinity if the values are located on the same line, while the RE method gives inadequate extrapolation for oscillatory convergence. To avoid incorrect extrapolation, it was decided to combine the two approaches and utilise AES for oscillating values and RE for monotone values. Thus, the resulting error is calculated as:

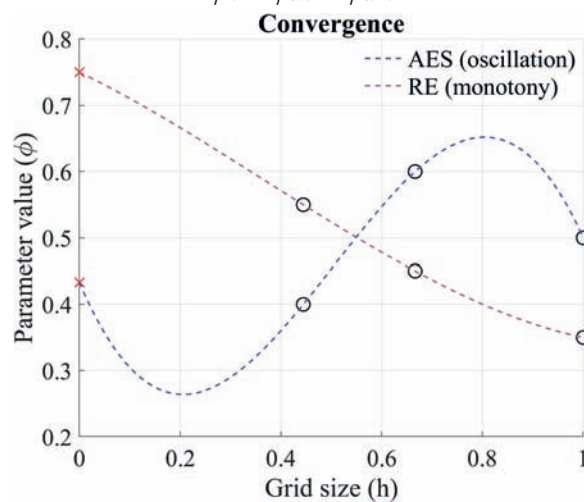
$$E_g = \begin{cases} GCI \cdot |\phi_h|, & (\phi_h - \phi_{\alpha h})(\phi_{\alpha h} - \phi_{\alpha^2 h}) > 0 \\ 3\sigma_\phi, & (\phi_h - \phi_{\alpha h})(\phi_{\alpha h} - \phi_{\alpha^2 h}) < 0 \end{cases} \quad (13)$$



(a) demonstration of RE failure for oscillatory convergence  $\phi_{\alpha h} < \phi_h, \phi_{\alpha^2 h}$  or  $\phi_{\alpha h} > \phi_h, \phi_{\alpha^2 h}$



(b) demonstration of AES failure for monotone convergence of  $\phi_h < \phi_{\alpha h} < \phi_{\alpha^2 h}$  or  $\phi_h > \phi_{\alpha h} > \phi_{\alpha^2 h}$



(c) correct operation of the methods  
Figure 8. Extrapolation examples

To evaluate the iteration convergence, the values sampled at the last 100 iterations were processed:

$$e_{it} = \left| \frac{\max(\phi_k) - \min(\phi_k)}{2 \text{mean}(\phi_k)} \right|, \quad (14)$$

where  $\phi_k$  are the values of an investigated variable at the  $k^{\text{th}}$  iteration ( $k = 601 \dots 700$ ).

For  $\text{mean}(\phi_k) \approx 0$ , the iteration error  $e_i$  takes very large values, not characterising convergence. In such cases, formula (14) is not applicable and the corresponding points are discarded.

## 2.5 Validation methods

When comparing the results of numerical and physical simulations, in addition to qualitative evaluations, the values of the validation metrics proposed in [8] were determined:

$$D_n = \frac{\sum_{j=1}^N |\phi_j^{efd} - \phi_j^{cfd}|}{\sum_{j=1}^N |\phi_j^{efd}|} \cdot 100\%; \quad (15)$$

$$R_{eq} = \frac{M}{N} \cdot 100\%, \quad (16)$$

where  $\phi_j^{efd}$ ,  $\phi_j^{cfd}$  are the iteratively averaged values of the investigated variables achieved from the physical and numerical modelling in the  $j^{\text{th}}$  control point, respectively;  $M$  is the number of control points with statistically coincident values;  $N$  is the total number of control points;  $D_n$  is the normalised deviation of the results; and  $R_{eq}$  is the fraction of the points

that match taking into account the error estimates or have a deviation of no more than 15%.

Metrics (11-12) are not subject to the disadvantage of the often-used  $R^2$  metric, which is insensitive to linear shifts.

In the current work, the following criteria for validation metrics are adopted:

$D_n \leq 15\%$  – good (green);

$15\% < D_n \leq 20\%$  – satisfactory (yellow);

$D_n > 20\%$  – not satisfactory (red);

$R_{eq} \geq 75\%$  – good (green);

$50\% \leq R_{eq} < 75\%$  – satisfactory (yellow);

$R_{eq} < 50\%$  – not satisfactory (red).

## 3. RESULTS AND DISCUSSION

This section presents the iteration and grid independence analyses results for the numerical solutions, and a comparison of the mean and peak pressure coefficients against the experimental data.

### 3.1 Iteration errors estimation

Iteration error can contribute significantly to the numerical solution error (Fig. 9).

The analysis shows that SST  $k-\omega$  has the worst iteration convergence, with  $e_{it}$  reaching 38% for some of the control points. The EARSM and GEKO models show significantly better convergence ( $e_{it} < 15\%$ ), and reducing the value of  $C_{SEP}$  leads to an even more improved convergence ( $e_{it} < 5\%$  for  $C_{SEP} = 1.25$ ).

For the most cases, refining the mesh reduces  $e_{it}$ , although this is not a general rule.

For all turbulence models, the influence of the surrounding buildings ( $180^\circ$ ) worsens the iteration convergence. This effect can be explained by the complexity of the flow structure.

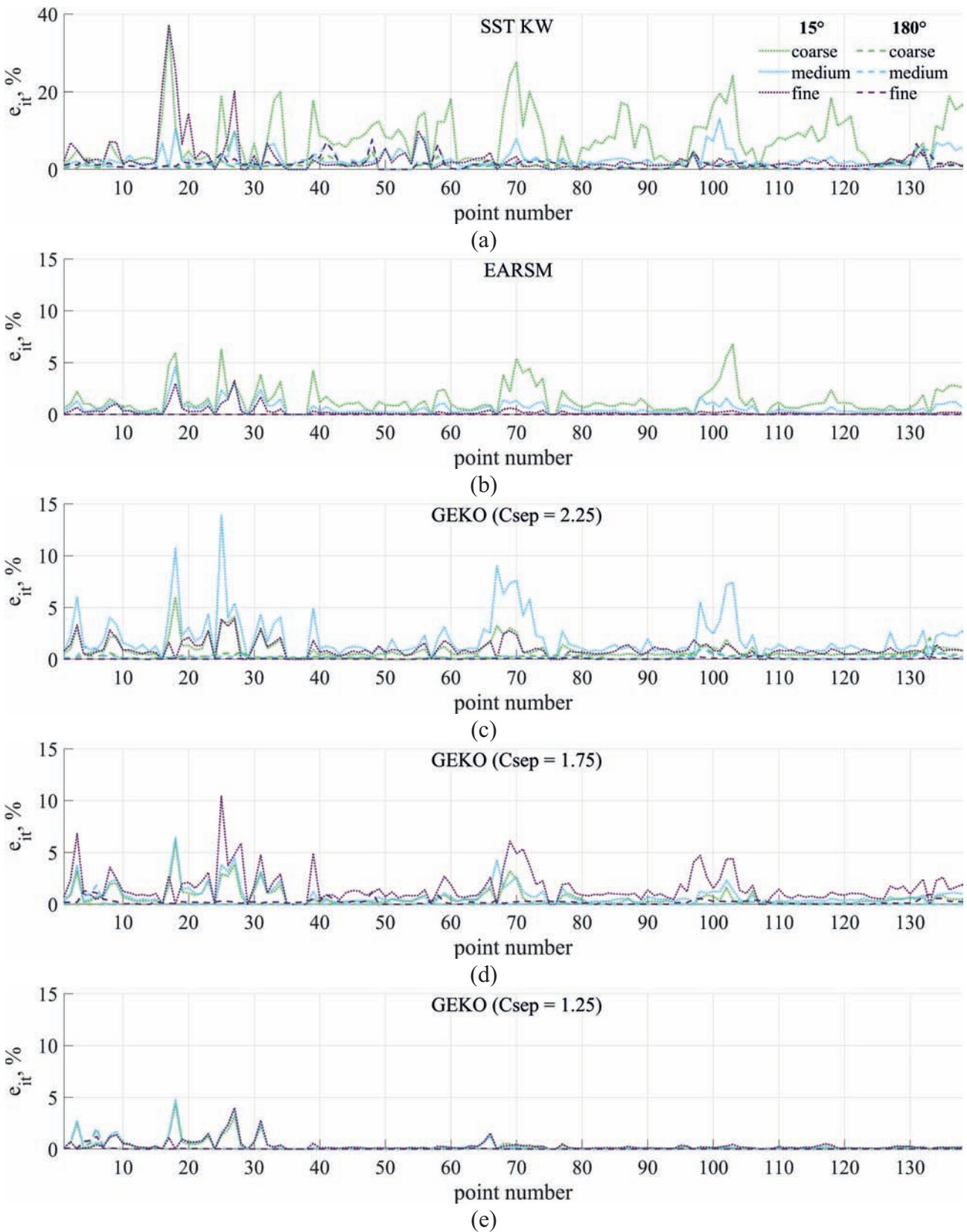


Figure 9. Iteration error  $e_{it}$  [%] for different turbulence models

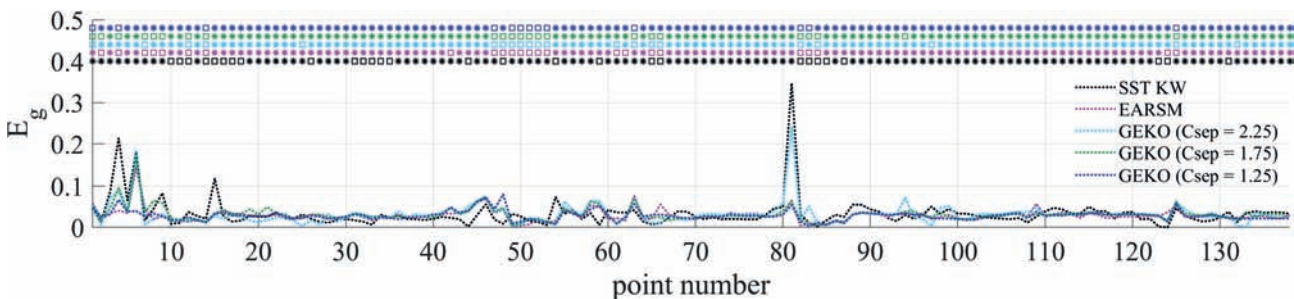
### 3.2 Grid errors estimation

Grid independence analysis using a combination of RE and AES methods (formula 13) resulted in plots of the absolute values of the errors  $E_g$  (Fig. 10).

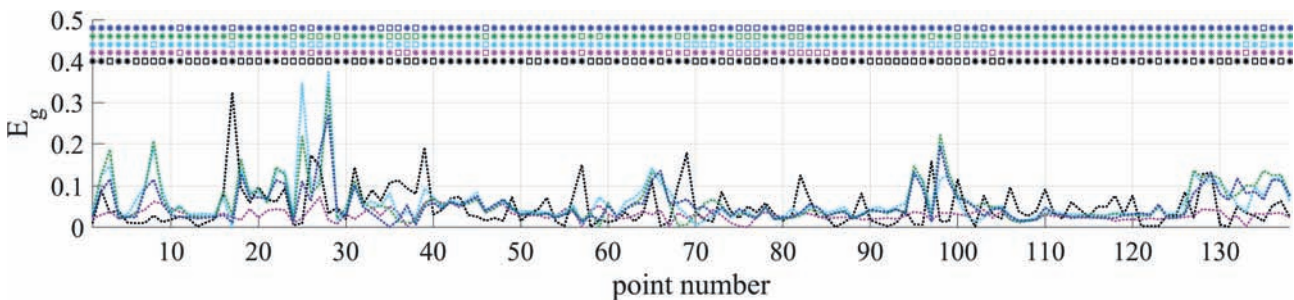
For all turbulence models, the influence of the surrounding buildings ( $180^\circ$ ) worsens the grid independence as well, which can be explained by the complication of the flow structure, too.

The solution for all turbulence models mostly demonstrates oscillatory behaviour (>80% of points).

The best grid independence was achieved with the EARSM model ( $E_g < 0.1$ ), followed by GEKO ( $C_{SEP} = 1.25$ ), while the worst results were obtained with GEKO ( $C_{SEP} = 2.25$ ) and SST ( $E_g < 0.4$ ) models.



(a)  $180^\circ$  (not influenced by the surrounding buildings)



(b)  $15^\circ$  (influenced by the surrounding buildings)

Figure 10. Grid error  $E_g$  for different turbulence models; the markers on the horizontal lines indicate the convergence behaviour:

\* – oscillatory;  $\square$  – monotone

### 3.3 CFD and EFD results comparison (validation)

Figures 11-13 show the comparison of mean and peak pressure coefficients from the numerical (with different turbulence models) and physical modelling. In the peak coefficient plots, the shaded areas (negative for  $c_{e,+}$  and

positive for  $c_{e,-}$ ) highlight values that are of no practical interest.

Table 1 summarises the values of the validation metrics (formulae 15-16). In calculating the validation metrics for peak coefficients, points in shaded areas were not considered.

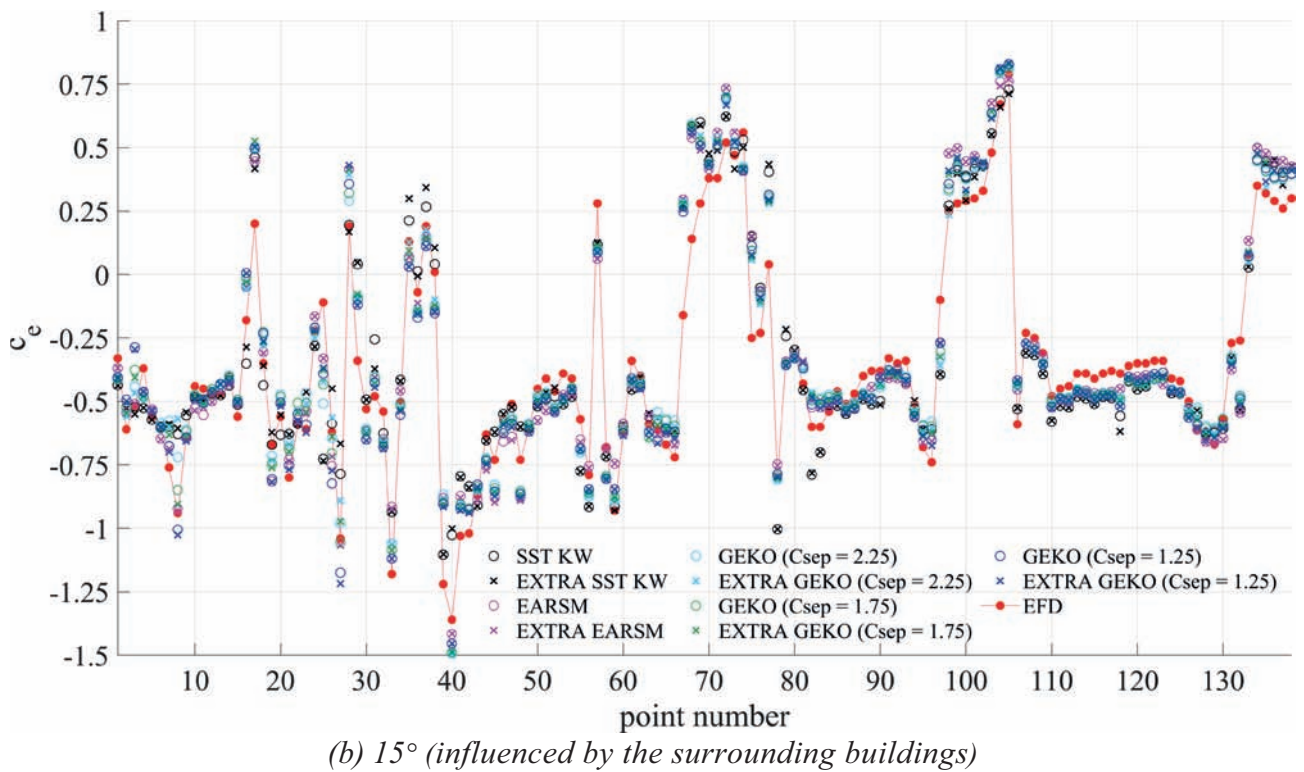
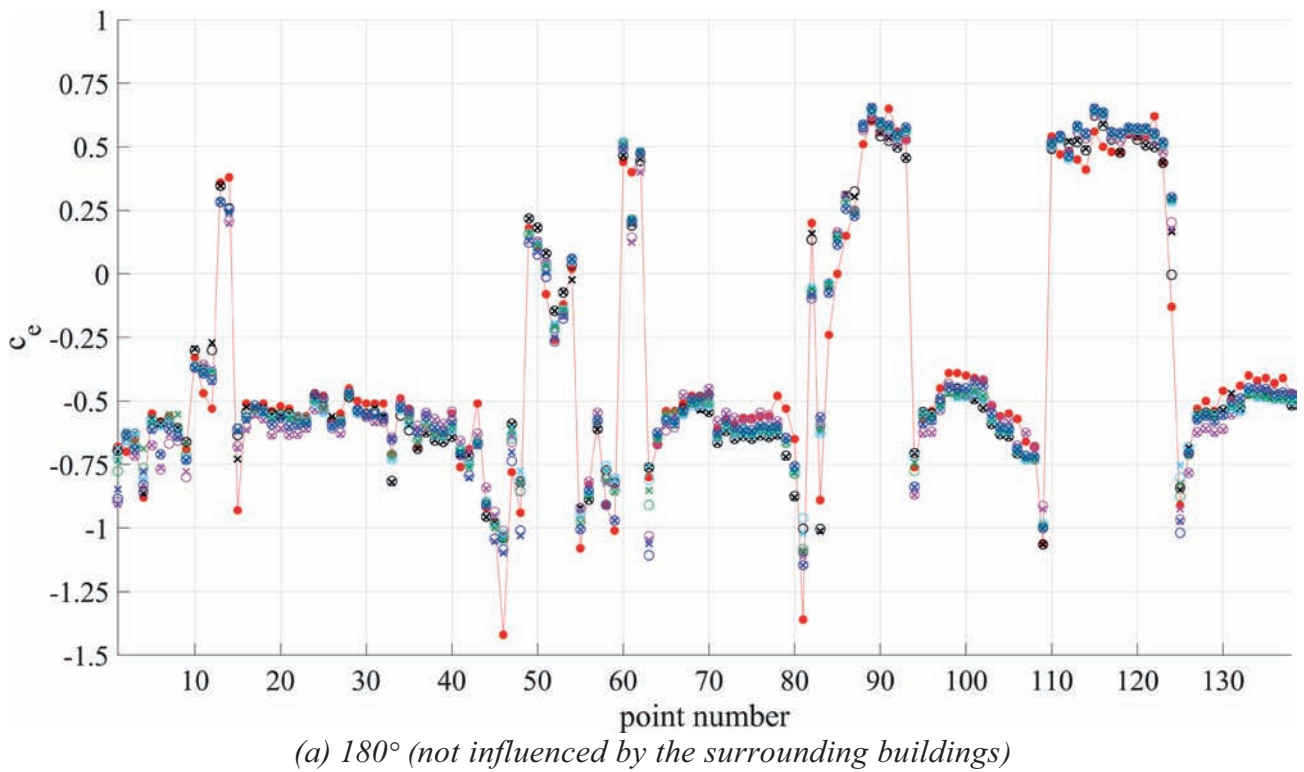


Figure 11. Comparison of mean pressure coefficients  $c_p$  for numerical and physical modelling

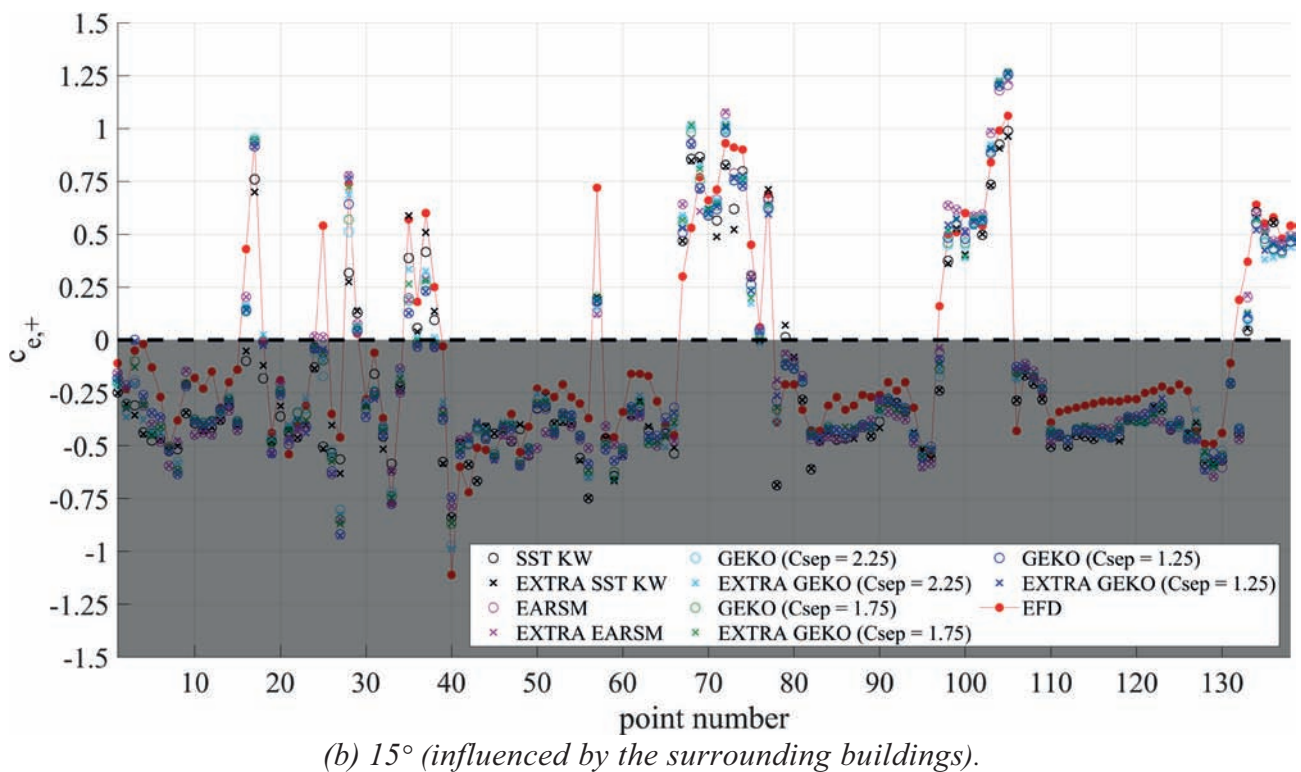
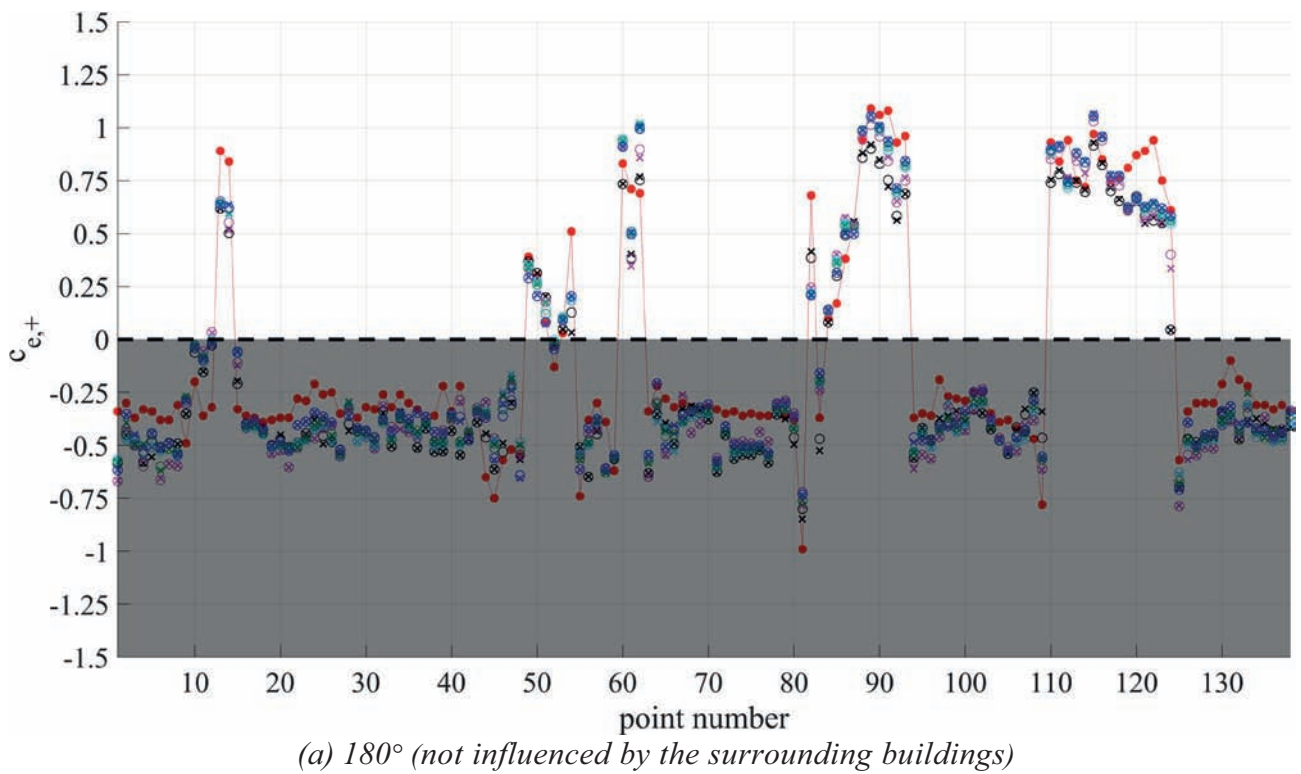


Figure 12. Comparison of positive peak pressure coefficients  $c_{e,+}$  for numerical and physical modelling

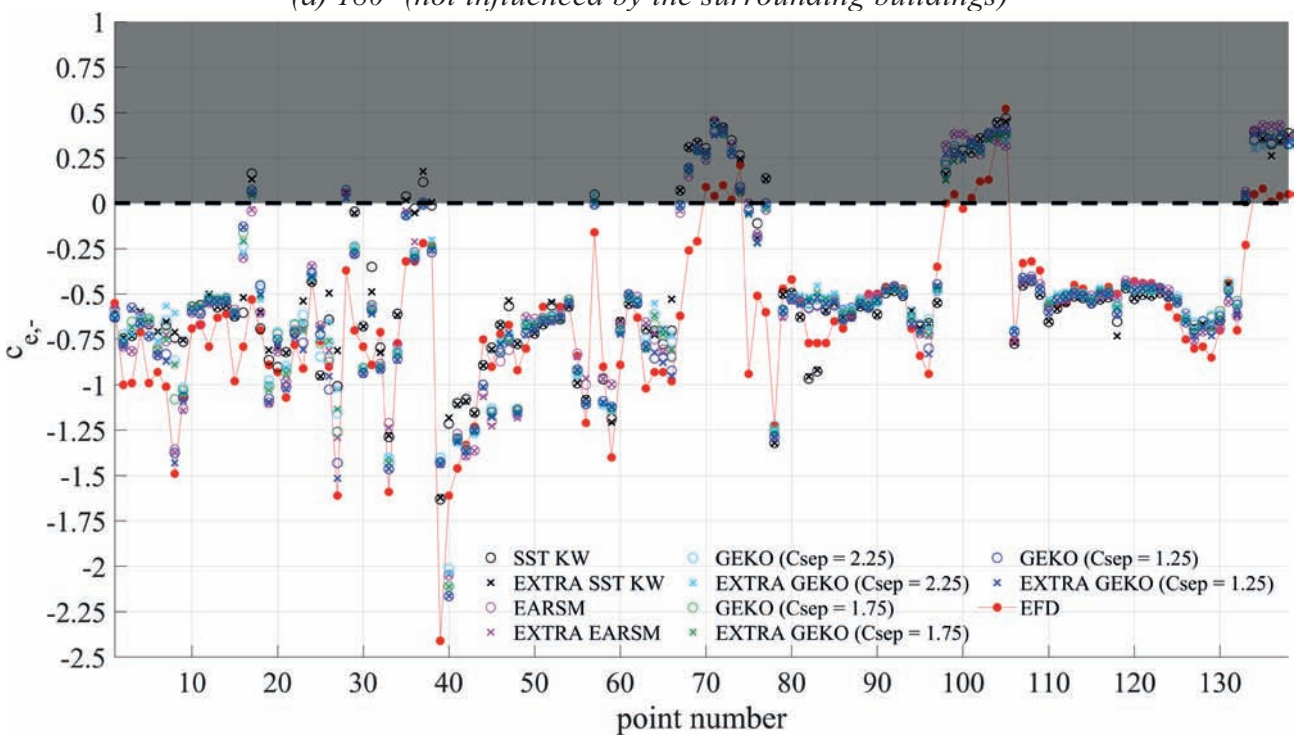
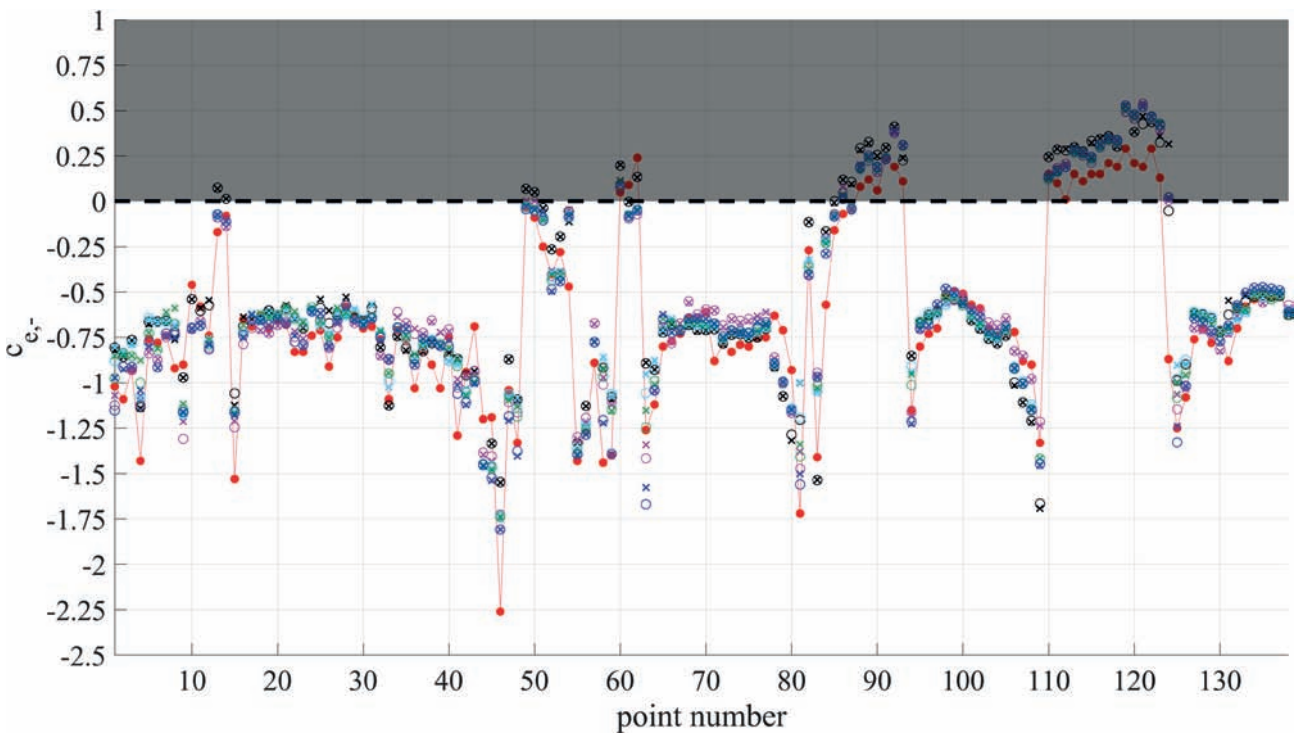


Figure 13. Comparison of negative peak pressure coefficients  $c_{e,-}$  for numerical and physical modelling

Table 1. Parameters of finite-volume meshes

$c$	Grid	15°		180°	
		$D_n, \%$	$R_{eq}, \%$	$D_n, \%$	$R_{eq}, \%$
SST $k-\omega$					
$C_e$	<i>ext</i>	22,66	42,75	12,56	65,94
	<i>fine</i>	22,25	40,57	12,33	68,11
	<i>med.</i>	22,62	47,82	14,08	68,84
	<i>coarse</i>	21,65	54,34	13,24	68,84
$C_{e,+}$	<i>ext</i>	34,00	48,64	24,37	36,11
	<i>fine</i>	33,79	45,94	24,28	36,11
	<i>med.</i>	36,80	48,64	21,44	38,88
	<i>coarse</i>	30,99	56,75	22,16	38,88
$C_{e,-}$	<i>ext</i>	27,48	40,49	20,07	46,08
	<i>fine</i>	26,36	41,32	19,29	46,95
	<i>med.</i>	25,54	48,76	18,48	55,65
	<i>coarse</i>	23,09	61,15	18,78	57,39
EARSM					
$C_e$	<i>ext</i>	20,36	59,42	14,21	75,36
	<i>fine</i>	20,29	64,49	14,16	77,53
	<i>med.</i>	21,80	65,94	15,31	81,88
	<i>coarse</i>	20,88	65,94	14,76	81,88
$C_{e,+}$	<i>ext</i>	30,92	56,75	22,43	44,44
	<i>fine</i>	29,72	64,86	22,37	44,44
	<i>med.</i>	30,32	64,86	21,76	47,22
	<i>coarse</i>	29,20	64,86	21,94	47,22
$C_{e,-}$	<i>ext</i>	22,86	58,67	16,31	71,30
	<i>fine</i>	22,35	67,76	16,08	73,04
	<i>med.</i>	21,75	70,24	15,48	76,52
	<i>coarse</i>	21,73	70,24	15,26	77,39
GEKO $k-\omega$ ( $C_{SEP} = 2.25$ )					
$C_e$	<i>ext</i>	19,35	66,66	13,15	83,33
	<i>fine</i>	19,60	70,28	12,90	84,05
	<i>med.</i>	21,11	70,28	14,06	84,05
	<i>coarse</i>	20,37	70,28	12,98	84,05
$C_{e,+}$	<i>ext</i>	32,30	64,86	20,75	55,55
	<i>fine</i>	33,09	70,27	20,52	61,11
	<i>med.</i>	31,27	70,27	20,12	61,11
	<i>coarse</i>	30,98	70,27	20,15	61,11
$C_{e,-}$	<i>ext</i>	24,80	69,42	18,08	75,65
	<i>fine</i>	24,39	74,38	17,53	82,60
	<i>med.</i>	22,49	74,38	16,61	82,60
	<i>coarse</i>	22,60	74,38	16,42	82,60

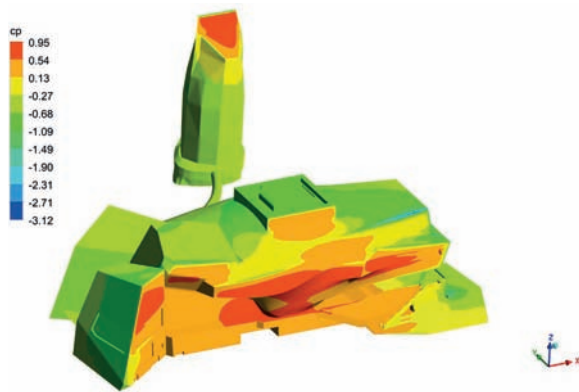
$c$	Grid	15°		180°	
		$D_n, \%$	$R_{eq}, \%$	$D_n, \%$	$R_{eq}, \%$
GEKO $k-\omega$ ( $C_{SEP} = 1.75$ )					
$C_e$	<i>ext</i>	19,40	65,21	12,70	81,88
	<i>fine</i>	19,56	70,28	12,34	84,05
	<i>med.</i>	21,59	70,28	13,87	84,05
	<i>coarse</i>	20,69	70,28	12,89	84,05
$C_{e,+}$	<i>ext</i>	30,74	62,16	20,24	55,55
	<i>fine</i>	32,04	70,27	19,97	61,11
	<i>med.</i>	30,77	70,27	19,57	61,11
	<i>coarse</i>	30,54	70,27	19,77	61,11
$C_{e,-}$	<i>ext</i>	23,28	69,42	16,96	75,65
	<i>fine</i>	23,37	74,38	16,11	82,60
	<i>med.</i>	21,75	74,38	15,25	82,60
	<i>coarse</i>	21,81	74,38	15,10	82,60
GEKO $k-\omega$ ( $C_{SEP} = 1.25$ )					
$C_e$	<i>ext</i>	19,71	64,49	12,21	81,15
	<i>fine</i>	19,78	69,56	12,03	83,33
	<i>med.</i>	22,75	69,56	13,86	84,05
	<i>coarse</i>	21,79	69,56	13,00	84,05
$C_{e,+}$	<i>ext</i>	31,51	62,16	19,18	55,55
	<i>fine</i>	31,22	64,86	19,36	58,33
	<i>med.</i>	30,16	70,27	19,06	61,11
	<i>coarse</i>	31,07	70,27	19,28	61,11
$C_{e,-}$	<i>ext</i>	20,84	69,42	14,90	75,65
	<i>fine</i>	21,56	72,72	14,86	79,13
	<i>med.</i>	20,59	74,38	14,74	82,60
	<i>coarse</i>	20,63	74,38	14,90	82,60

The results show that the GEKO  $k-\omega$  model with  $C_{SEP} = 1.25$  showed the best fit to the experimental data. In contrast, the widely used SST  $k-\omega$  model showed the worst fit.

For all the models, the cases without the influence of the surrounding buildings (180°) show significantly better fits to the experimental data than the ones accounting for it (15°).

### 3.4 Results visualisation

To better understand the flow regimes in the domain, the contours of the mean pressure coefficients and mean flow velocity obtained for the SST  $k-\omega$  (coarse grid) model are presented.



(a) 180° (windward)



(b) 180° (leeward)

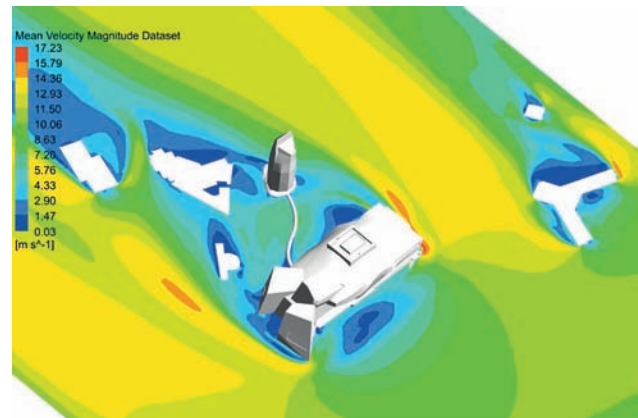


(c) 15° (windward)

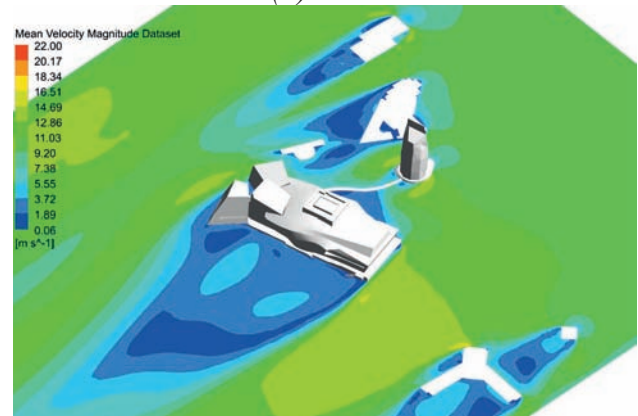


(d) 15° (leeward)

Figure 14. Mean pressure coefficient  $c_e$



(a) 180°



(b) 15°

Figure 15. Mean flow velocity at 0.045 m

#### 4. CONCLUSIONS

The following conclusions are made from the conducted research:

1. Numerical models of a unique facility, the MTEC in Kemerovo, and the surrounding buildings have been developed in Ansys Fluent. A total of 2 wind directions (with and without the influence of the buildings), 3 levels of mesh detailing (3.1, 5.6, 12.8 million cells) and 5 turbulence models (SST  $k-\omega$ , EARSM, GEKO  $k-\omega$  ( $C_{SEP} = 1.25, 1.75, 2.25$ )) were considered.

2. A thorough **verification** has been carried out to investigate the iteration and grid independence of the solution:

- Iteration and grid error can contribute significantly to the numerical solution results. To minimise this effect, it is necessary to use iterative averaging and improve the mesh quality for the bad areas.

- The often recommended methods for extrapolating the solution to an infinitesimal mesh cannot simply be applied in general. Richardson extrapolation may give inadequate predictions for oscillatory convergence, while the approximate error spline may fail for monotone convergence.

- For all turbulence models, the influence of the surrounding buildings negatively impacts the iteration and grid independence of the solution. This effect can be explained by the complexity of the flow structure.

- The solution for all the turbulence models mostly (>80% of the points) demonstrates oscillatory behaviour on different meshes.

- It has been found that the SST  $k-\omega$  show the worst iteration and grid independence among the studied models.

- The EARSM and GEKO models show significantly better iteration independence ( $e_{it} < 15\%$ ), and decreasing the  $C_{SEP}$  further improves it ( $e_{it} < 5\%$  for  $C_{SEP} = 1.25$ ).

- The best grid independence is achieved for the EARSM model ( $E_g < 0.1$ ), followed by GEKO ( $C_{SEP} = 1.25$ ), and the worst for GEKO ( $C_{SEP} = 2.25$ ) and SST ( $E_g < 0.4$ ).

**3.** A thorough **validation** has been carried out, which is a comparison of the numerical (CFD) and physical (WT) modelling results using the special metrics  $D_n$  and  $R_{eq}$ .

- The application of RE and AES extrapolation methods did not lead to a systematic improvement of the results (the fit with experiment), so these methods are not recommended the validation of structural aerodynamics problems.

- For all the turbulence models, the influence of the surrounding building negatively impacts the fit to the experiment. This effect can be explained by the complexity of the flow structure.

- The GEKO  $k-\omega$  turbulence model with the parameter  $C_{SEP} = 1.25$  showed a significantly better fit to the experimental data for both mean and peak pressure coefficients' values. This model is recommended for use in wind loads determination for relatively low buildings (meaning their

height is less than both their width and length) in steady-state simulations.

**4.** It is confirmed that Ansys Fluent allows the mean and peak wind loads determination on buildings of complex shape with the accuracy sufficient enough for practical purposes, provided that modern turbulence models and methods set out in the STO [15] are used.

## ACKNOWLEDGEMENTS

The research was conducted as part of the development programme for 2025-2036 of Moscow State University of Civil Engineering under the framework of strategic academic leadership programme "Priority 2030".

## REFERENCES

1. **Cochran L.** State of the art review of wind tunnels and physical modelling to obtain structural loads and cladding pressures // Architectural Science Review. – 2006. – Vol. 49. – No. 1. – Pp. 7-16.
2. **Cermak J. E.** Wind-tunnel development and trends in applications to civil engineering // J. Wind Eng. Ind. Aerodyn. – 2003. – Vol. 91. – No. 3. – Pp. 355-370.
3. **Li Y., Zhu Y., Chen F. B., Li Q. S.** Aerodynamic loads of tapered tall buildings: Insights from wind tunnel test and CFD // Structures. – 2023. – Vol.56. – PaperID 104975.
4. **Dubinsky S.I.** Numerical modeling of wind impacts on high-rise buildings and complexes: Dissertation for the degree of Candidate of Technical Sciences. Moscow, 2010. – 198 p. (In Russ.)
5. **Doroshenko A.V.** Methodology for numerical modeling of wind speeds and pedestrian comfort in residential areas: Dissertation for the degree of Candidate of Technical Sciences. Moscow, 2013. – 169 p. (In Russ.)

6. **Britikov N.A.** Numerical modeling of snow loads on roofs of large-span buildings and structures: Dissertation for the degree of Candidate of Technical Sciences. Moscow, 2023. – 150 p. (In Russ.)
7. **Afanasyeva I.N.** Adaptive methodology for numerical modeling of three-dimensional dynamic problems of structural aerohydroelasticity: Dissertation for the degree of Candidate of Technical Sciences. Moscow, 2014. – 200 p. (In Russ.)
8. **Goryachevsky O.S.** Dynamic analysis of flexible façade structures under numerically simulated wind loads: Dissertation for the degree of Candidate of Technical Sciences. Moscow, 2024. – 210 p. (In Russ.)
9. **Saiyan S.G., Efimova A.M.** Computational aerodynamic studies of the MIBC “Moscow-City” complex during sequential construction of buildings // Vestnik MSUCE. – 2024. – Vol. 19. – No. 6. – Pp. 906-941. (In Russ.)
10. **Belostotsky A.M., Akimov P.A., Afanas'eva I.N.** Vychislitel'naya aerodinamika v zadachah stroitel'stva, M.: Izdatel'stvo ASV. – 2017. – 720 p. (In Russ.)
11. **Thordal M. S., Bennetsen J. C., Capra S., Koss H. H. H.** Towards a standard CFD setup for wind load assessment of high-rise buildings: Part 1–Benchmark of the CAARC building // J. Wind Eng. Ind. Aerodyn.. – 2020. – Vol.205. – PaperID 104283.
12. **Wang X. J., Li Q. S., Yan B. W.** Full-scale measurements of wind pressures on a low-rise building during typhoons and comparison with wind tunnel test results and aerodynamic database // J. of Struct. Eng. – 2020. – Vol.146. – PaperID 04020196.
13. **Lamberti G., Gorlé C.** A multi-fidelity machine learning framework to predict wind loads on buildings // J. Wind Eng. Ind. Aerodyn.. – 2021. – Vol.214. – PaperID 104647.
14. **Saiyan S.G., Shitikova M.V.** Analysis of wind loads and impacts on high-rise buildings and structures. Review of the current state, challenges, and prospects. Part 1. Wind loads and methods for their determination. News of Higher Educational Institutions. Construction. – 2025. – No. 4. – Pp. 5–19. (In Russ.)
15. STO 02066523-089-1-2024. Numerical modelling of wind and snow actions.
16. **Goryachevsky O.S.** Numerical modelling of wind loads on windows. Validation for a high-rise square plan building // J. Comput. Civ. Struct. Eng. – 2023. – Vol. 19. – No. 3. – Pp. 114–129.
17. GOST R 57188–2016 Numerical modeling of physical processes. Terms and definitions. (In Russ.)
18. ASME V&V 20–2009 Standard for Verification and Validation in Computational Fluid Dynamics and Heat Transfer
19. **Celik I. B., Ghia U., Roache P. J., Freitas C. J.** Procedure for Estimation and Reporting of Uncertainty Due to Discretization in CFD Applications // J. Fluids Eng. – 2008. – Vol. 130. – No.7. – PaperID 078001.
20. **Franke J.** Best practice guideline for the CFD simulation of flows in the urban environment // COST Office Brussels. – 2007. – ISBN: 3-00-018312-4.
21. **Tominaga Y., Mochida A., Yoshie R., Kataoka H., Nozu T., Yoshikawa M., et al.** AIJ guidelines for practical applications of CFD to pedestrian wind environment around building // J. Wind Eng. Ind. Aerodyn. – 2008. – Vol. 96. – pp. 1749-1761.
22. **Roache P.J.** Verification and Validation in Computational Science and Engineering // Hermosa Publishers,

- Albuquerque, New Mexico – 1998. – p. 446.
23. **Freitas C. J.** Journal of fluids engineering editorial policy statement on the control of numerical accuracy // *J. Fluids Eng.* – 1986. – Pp. 339-340.
  24. **Celik I., Karatekin O.** Numerical Experiments on Application of Richardson Extrapolation With Nonuniform Grids // *J. Fluids Eng.* – 1997. Vol. 119. – No. 3. – Pp. 584-590.
  25. **Celik I., Karaismail E., Parsons D. A.** Reliable Error Estimation Technique for CFD Applications // AVT-147 Symposium on Computational Uncertainty in Military Vehicle Design – 2007. – PaperID RTO-MP-AVT-147
  26. **Roache P. J.** Perspective: A Method for Uniform Reporting of Grid Refinement Studies // *J. Fluids Eng.* – 1994. – Vol. 116. – No. 3. – Pp. 405-413.
  27. **Roache P. J.** Quantification of uncertainty in computational fluid dynamics // *Annu. Rev. Fluid Mech.* – 1997. Vol. 29. – No. 1. – Pp. 123-160.
  28. Regulation on the verification of software tools used to determine loads and impacts, stress-strain (and other) states, dynamic characteristics, and to assess the strength, stability, and safety of structures, buildings, and facilities / RAASN // Approved by the Presidium of RAASN, Protocol No. 11 of November 25, 2016. – Moscow, 2016. – 28 p. (In Russ.)
  29. Ansys Fluent Theory Guide. Release 2024 R1. // Canonsburg: ANSYS Inc. – 2021. – p. 1320.
  1. **Cochran L.** State of the art review of wind tunnels and physical modelling to obtain structural loads and cladding pressures // *Architectural Science Review.* – 2006. – Vol. 49. – No. 1. – Pp. 7-16.
  2. **Cermak J. E.** Wind-tunnel development and trends in applications to civil engineering // *J. Wind Eng. Ind. Aerodyn.* – 2003. – Vol. 91. – No. 3. – Pp. 355-370.
  3. **Li Y., Zhu Y., Chen F. B., Li Q. S.** Aerodynamic loads of tapered tall buildings: Insights from wind tunnel test and CFD // *Structures.* – 2023. – Vol.56. – PaperID 104975.
  4. **Дубинский С.И.** Численное моделирование ветровых воздействий на высотные здания и комплексы: диссертация на соискание ученой степени кандидата технических наук. – Москва, 2010. – 198 с.
  5. **Дорошенко А.В.** Методика численного моделирования скоростей ветра и пешеходной комфортности в зонах жилой застройки: диссертация на соискание ученой степени кандидата технических наук. – Москва, 2013. – 169 с.
  6. **Бритиков Н.А.** Численное моделирование снеговых нагрузок на покрытия большепролетных зданий и сооружений: диссертация на соискание ученой степени кандидата технических наук. – Москва, 2023. – 150 с.
  7. **Афанасьева И.Н.** Адаптивная методика численного моделирования трехмерных динамических задач строительной аэрогидроупругости: диссертация на соискание ученой степени кандидата технических наук. – Москва, 2014. – 200 с.
  8. **Горячевский О.С.** Динамический расчет гибких фасадных конструкций на численно моделируемые ветровые воздействия: диссертация на соискание ученой степени кандидата технических наук. – Москва, 2024. – 210 с.
  9. **Сайян С.Г., Ефимова А.М.** Расчетные аэродинамические исследования комплекса Московского

## СПИСОК ЛИТЕРАТУРЫ

1. **Cochran L.** State of the art review of wind tunnels and physical modelling to obtain structural loads and cladding pressures

- международного делового центра «Москва-Сити» при последовательном возведении зданий // Вестник МГСУ. – 2024. – Т. 19, № 6. – С. 906-941.
10. **Белостоцкий А.М., Акимов П.А., Афанасьева И.Н.** Вычислительная аэродинамика в задачах строительства, М.: Издательство АСВ, 2017, 720 с.
  11. **Thordal M. S., Bennetsen J. C., Capra S., Koss H. H. H.** Towards a standard CFD setup for wind load assessment of high-rise buildings: Part 1 – Benchmark of the CAARC building // *J. Wind Eng. Ind. Aerodyn.* – 2020. – Vol.205. – PaperID 104283.
  12. **Wang X. J., Li Q. S., Yan B. W.** Full-scale measurements of wind pressures on a low-rise building during typhoons and comparison with wind tunnel test results and aerodynamic database // *J. of Struct. Eng.* – 2020. – Vol.146. – PaperID 04020196.
  13. **Lamberti G., Gorlé C.** A multi-fidelity machine learning framework to predict wind loads on buildings // *J. Wind Eng. Ind. Aerodyn.* – 2021. – Vol.214. – PaperID 104647.
  14. **Саиян С.Г., Шитикова М.В.** Анализ ветровых нагрузок и воздействий на высотные здания и сооружения. Обзор современного состояния, проблемы и перспективы. Часть 1. Ветровые нагрузки и методы их определения // *Известия вузов. Строительство.* – 2025. – № 4. – С. 5-19.
  15. СТО 02066523-089-1-2024. Численное моделирование ветровых и снеговых воздействий.
  16. **Горячевский О.С.** Численное моделирование ветровых давлений на окна. Валидация для типового многоэтажного здания квадратной формы // *J. Comput. Civ. Struct. Eng.* – 2023. – Том. 19. – №. 3. – с. 114–129.
  17. ГОСТ Р 57188–2016 Численное моделирование физических процессов. Термины и определения.
  18. ASME V&V 20–2009 Standard for Verification and Validation in Computational Fluid Dynamics and Heat Transfer
  19. **Celik I. B., Ghia U., Roache P. J., Freitas C. J.** Procedure for Estimation and Reporting of Uncertainty Due to Discretization in CFD Applications // *J. Fluids Eng.* – 2008. – Vol. 130. – No.7. – PaperID 078001.
  20. **Franke J.** Best practice guideline for the CFD simulation of flows in the urban environment // COST Office Brussels. – 2007. – ISBN: 3-00-018312-4.
  21. **Tominaga Y., Mochida A., Yoshie R., Kataoka H., Nozu T., Yoshikawa M., et al.** AIJ guidelines for practical applications of CFD to pedestrian wind environment around building // *J. Wind Eng. Ind. Aerodyn.* – 2008. – Vol. 96. – pp. 1749-1761.
  22. **Roache P.J.** Verification and Validation in Computational Science and Engineering // Hermosa Publishers, Albuquerque, New Mexico – 1998. – p. 446.
  23. **Freitas C. J.** Journal of fluids engineering editorial policy statement on the control of numerical accuracy // *J. Fluids Eng.* – 1986. – Pp. 339-340.
  24. **Celik I., Karatekin O.** Numerical Experiments on Application of Richardson Extrapolation With Nonuniform Grids // *J. Fluids Eng.* – 1997. Vol. 119. – No. 3. – Pp. 584-590.
  25. **Celik I., Karaismail E., Parsons D. A.** Reliable Error Estimation Technique for CFD Applications // AVT-147 Symposium on Computational Uncertainty in Military Vehicle Design – 2007. – PaperID RTO-MP-AVT-147
  26. **Roache P. J.** Perspective: A Method for Uniform Reporting of Grid Refinement

- Studies // J. Fluids Eng. – 1994. – Vol. 116. – No. 3. – Pp. 405-413.
27. **Roache P. J.** Quantification of uncertainty in computational fluid dynamics // Annu. Rev. Fluid Mech. – 1997. Vol. 29. – No. 1. – Pp. 123-160.
28. Положение о верификации программных средств, применяемых при определении нагрузок и воздействий, напряженно-деформированного (и иного) состояния, динамических характеристик, оценке прочности, устойчивости и безопасности конструкций, зданий и сооружений / РААСН // Утв. президиумом РААСН, протокол №11 от 25 нояб. 2016 г. – М., 2016. – 28 с.
29. Ansys Fluent Theory Guide. Release 2024 R1. // Canonsburg: ANSYS Inc. – 2021. – p. 1320.

---

*Alexander Mikhailovich Belostotsky* – DSc, Professor, Full Member of the Russian Academy of Architecture and Construction Sciences, General Director R&D Centre StaDyO; 125040, Russia, Moscow, 3ya Ulitsa Yamskogo Polya, 18. Scientific adviser at A.B. Zolotov REC CM of the National Research Moscow State University of Civil Engineering; 129337, Russia, Moscow, Yaroslavskoe shosse, 26. e-mail: amb@stadyo.ru

*Александр Михайлович Белостоцкий* – генеральный директор АО НИЦ СтаДиО; 125040, Россия, Москва, 3-я улица Ямского поля, 18. Научный руководитель НОЦ КМ им. А.Б. Золотова Национального исследовательского Московского государственного строительного университета; 129337, Россия, г. Москва, Ярославское шоссе, д. 26. e-mail: amb@stadyo.ru

*Oleg Sergeevich Goryachevsky* – CSc, Deputy Director at A.B. Zolotov REC CM of the National Research Moscow State University of Civil Engineering; 129337, Russia, Moscow, Yaroslavskoe shosse, 26. Leading engineer of R&D Centre StaDyO; 125040, Russia, Moscow, 3ya Ulitsa Yamskogo Polya, 18. e-mail: osg@reccm.ru

*Олег Сергеевич Горячевский* – к.т.н., заместитель директора НОЦ КМ им. А.Б. Золотова Национального исследовательского Московского государственного строительного университета; 129337, Россия, г. Москва, Ярославское шоссе, д. 26. Ведущий инженер-расчетчик АО НИЦ СтаДиО; 125040, Россия, г. Москва, 3-я улица Ямского поля, 18 e-mail: osg@reccm.ru

*Sergey Gurgenovich Saiyan* – Researcher at A.B. Zolotov REC CM of the National Research Moscow State University of Civil Engineering; 129337, Russia, Moscow, Yaroslavskoe shosse, 26. e-mail: berformert@gmail.com

*Сергей Гургенович Саиян* – научный сотрудник НОЦ КМ им. А.Б. Золотова Национального исследовательского Московского государственного строительного университета; 129337, Россия, г. Москва, Ярославское шоссе, д. 26. e-mail: berformert@gmail.com

*Efimova Alexandra Mikhailovna* – leading research engineer at LLC «ТМН Advance Technology Center»; 121205, Russia, Moscow, Skolkovo, Nobel str. 7 e-mail: sasha.basket.8@yandex.ru

*Ефимова Александра Михайловна* – ведущий инженер-исследователь ООО «Центр Перспективных Технологий ТМХ»; 121205, г. Москва, тер. Сколково Инновационного центра, ул. Нобеля, д. 7 e-mail: sasha.basket.8@yandex.ru